

Design of High Speed VLSI Architecture for 1-D Discrete Wavelet Transform

Rashmi Patil¹, Dr. M. T. Kolte²

¹Research Student, Department of Electronics, B. D. C. O. E., Wardha, Maharashtra, India

²Professor and H. O. D. of ENTC Department, India M. I. T. C. O. E., Pune, Maharashtra, India

Abstract: The work presents an implementation of discrete wavelet transform (DWT) using systolic array architecture in VLSI. The architecture consists of filter unit, storage unit and control unit. This performs calculations of low pass and high pass coefficients by using only one multiplier. This architecture has been implemented and simulated using VLSI. The hardware utilization efficiency is more as compared to the referred due to the FBRA scheme. The systolic nature of this architecture corresponds to a clock speed of 19.27MHz for Coiflets1 wavelet as compared to other two wavelets. It has advantage for optimizing area and time. The architecture is modular and cascadable for one or multi-dimensional DWT.

Keywords: DWT, FRA, hardware efficiency, six tap Fir Filter, Systolic Array

1. Introduction

In the last decade, there has been an enormous increase in the applications of wavelets in various scientific disciplines to relate the discrete-time filter bank with the theory of continuous time function space. Typical applications of wavelets include signal processing, image processing, numerical analysis, statistics, biomedicine, etc.[1], [2]. Wavelet transform offers a wide variety of useful features, in contrast to other transforms, such as Fourier transform or cosine transform. Some of these are as follows:

- Computational complexity of $O(N)$, where N is the number of data samples [3]
- Efficient VLSI implementation [4]
- Low computational complexity, flexibility in representing non stationary image signals

Redundancies in video sequence can be removed by using Discrete Cosine Transform (DCT). DCT suffers from the negative effects of blackness and mosquito noise resulting in poor subjective quality of reconstructed images at high compression [5]. In order to meet the real time requirements in many applications, design and implementation of DWT is required [6], [7].

2. Discrete Wavelet Transform

DWT which is based on sub band coding, is fast computation wavelet transform. It is easy to implement and reduces the computation time and resources required. Wavelets can be realized by iteration of filters with scaling. The resolution of the signal, which is a measure of the amount of detail information in the signal, is determined by the filtering operations, and the scale is determined by upsampling and down sampling (subsampling) operations [2].

A schematic of three stage DWT decomposition is shown in Figure 1.

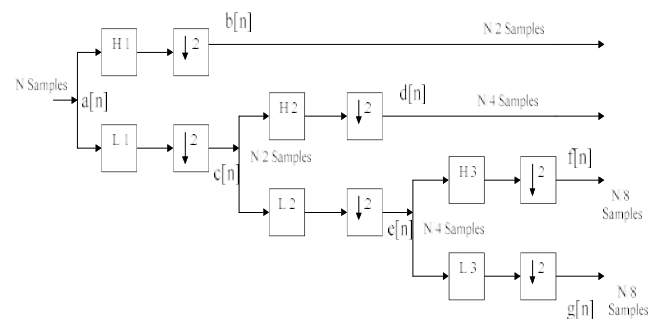


Figure 1: Three Stage DWT Decomposition using Pyramid Algorithm

In Figure 1, the signal is denoted by the sequence $a[n]$, where n is an integer. The low pass filter is denoted by $L1$ while the high pass filter is denoted by $H1$. At each level, the high pass filter produces detail information $b[n]$, while the low pass filter associated with scaling function produces coarse approximation $c[n]$.

Here the input signal $a[n]$ has N samples. At the first decomposition level, the signal is passed through the high pass and low pass filters, followed by sub sampling by 2. The output of the high pass filter has $N/2$ samples and $b[n]$. These $N/2$ samples constitute the first level of DWT coefficients. The output of the low pass filter also has $N/2$ samples and $c[n]$. The signal is then passed through low pass and high pass filters for further decomposition. The output of the second low pass filter followed by sub sampling has $N/4$ samples and $e[n]$. The output of the second high pass filter followed by sub sampling has $N/4$ samples and $d[n]$. The second high pass filter constitutes the second level of DWT coefficients. The low pass filter output is then filtered once again for further decomposition and produces $g[n]$, $f[n]$ with $N/8$ samples. The filtering and decimation process is continued until the desired level is reached. The maximum number of levels depends on the length of the signal.

3. Data Dependencies within DWT

The wavelet decomposition of a 1-D input signal for three stages is shown in Figure 1. The transfer functions of the sixth order high pass (g(n)) and low pass h(n) filter can be expressed as follows:

$$\begin{aligned} \text{High}(z) &= g_0 + g_1z^{-1} + g_2z^{-2} + g_3z^{-3} + g_4z^{-4} + g_5z^{-5} & (1a) \\ \text{Low}(z) &= h_0 + h_1z^{-1} + h_2z^{-2} + h_3z^{-3} + h_4z^{-4} + h_5z^{-5} & (1b) \end{aligned}$$

For clarity the intermediate and final DWT coefficients in Figure 1 are denoted by a, b, c, d, e, f, and g. The DWT computations are complex because of the data dependencies at different octaves. Equations 2a-2n shows the relationship among a, b, c, d, e, f, and g.

1st octave:

$$b(0) = g(0)a(0) + g(1)a(-1) + g(2)a(-2) + g(3)a(-3) + g(4)a(-4) + g(5)a(-5) \quad (2a)$$

$$b(2) = g(0)a(2) + g(1)a(1) + g(2)a(0) + g(3)a(-1) + g(4)a(-2) + g(5)a(-3) \quad (2b)$$

$$b(4) = g(0)a(4) + g(1)a(3) + g(2)a(2) + g(3)a(1) + g(4)a(0) + g(5)a(-1) \quad (2c)$$

$$b(6) = g(0)a(6) + g(1)a(5) + g(2)a(4) + g(3)a(3) + g(4)a(2) + g(5)a(1) \quad (2d)$$

$$c(0) = h(0)a(0) + h(1)a(-1) + h(2)a(-2) + h(3)a(-3) + h(4)a(-4) + h(5)a(-5) \quad (2e)$$

$$c(2) = h(0)a(2) + h(1)a(1) + h(2)a(0) + h(3)a(-1) + h(4)a(-2) + h(5)a(-3) \quad (2f)$$

$$c(4) = h(0)a(4) + h(1)a(3) + h(2)a(2) + h(3)a(1) + h(4)a(0) + h(5)a(-1) \quad (2g)$$

$$c(6) = h(0)a(6) + h(1)a(5) + h(2)a(4) + h(3)a(3) + h(4)a(2) + h(5)a(1) \quad (2h)$$

2nd octave:

$$d(0) = g(0)c(0) + g(1)c(-2) + g(2)c(-4) + g(3)c(-6) + g(4)c(-8) + g(5)c(-10) \quad (2i)$$

$$d(4) = g(0)c(4) + g(1)c(2) + g(2)c(0) + g(3)c(-2) + g(4)c(-4) + g(5)c(-6) \quad (2j)$$

$$e(0) = h(0)c(0) + h(1)c(-2) + h(2)c(-4) + h(3)c(-6) + h(4)c(-8) + h(5)c(-10) \quad (2k)$$

$$e(4) = h(0)c(4) + h(1)c(2) + h(2)c(0) + h(3)c(-2) + h(4)c(-4) + h(5)c(-6) \quad (2l)$$

3rd octave:

$$f(0) = g(0)e(0) + g(1)e(-4) + g(2)e(-8) + g(3)e(-12) + g(4)e(-16) + g(5)e(-20) \quad (2m)$$

$$g(0) = h(0)e(0) + h(1)e(-4) + h(2)e(-8) + h(3)e(-12) + h(4)e(-16) + h(5)e(-20) \quad (2n)$$

4. Systolic Array (SA) Architecture for DWT

The design of DWT-SA is based on computation schedule derived from Equations 2a-2n, which are the result of

applying the pyramid algorithm for N=8 to the sixstage filter.

As shown in Equations 2a-2n there are eight first octave coefficients computations, four second octave coefficients and two third octave computations. The DWT-SA architecture comprises of the following basic blocks:

- 4.1. The Filter Unit (FU)
- 4.2. The Storage Unit
- 4.3. The Control Unit (CU)

4.1. The Filter Unit (FU)

Equations 1a-1b show that the high pass and low pass filter coefficients can be computed using a six stage multiply and accumulate digital filter, where partial results are computed at each stage separately and then progressively passed to the next higher stage for accumulation. Equations 1a-1b suggests that due to filter coefficient calculations spanning over 5 clock cycles, a temporary storage is required for the incoming data samples.

The filter unit proposed for this architecture is a six-stage non-recursive FIR digital filter whose transfer functions for the high-pass and low-pass components are shown in Equations 2a-2n. The systolic architecture of a six-stage filter is shown in Figure-2. The latency of each filter stage is 1.

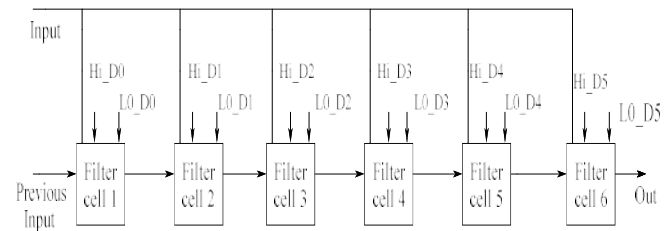


Figure 2: Systolic architecture of a six-stage filter

The filter behaves in a systolic manner by computing partial products of more than one coefficient at a time. The first multiply and accumulate stage computes the first partial product and passes it to the second filter stage where it is added to the second partial product. That repetitive action continues until a complete DWT coefficient is out from the sixth filter stage.

The filter consists of band select signal. If band selects is '1' then it selects low pass coefficients. If band selects '0' then it selects high pass coefficients. The partial results are passed synchronously in a systolic manner from one cell to the adjacent cell. The filter cell consist therefore of only one multiplier, one adder and two registers to store high pass and low pass coefficients. The RTL schematic of filter unit is shown in Figure 3.

In filter cell, a signed number multiplication problem occurs. The signed-number represents either positive, negative numbers or one positive and other negative numbers. To avoid this problem, the proposed filter cell consists of invert and xor operation as shown in Figure 4. The RTL schematic of filter cell is shown in Figure 5.

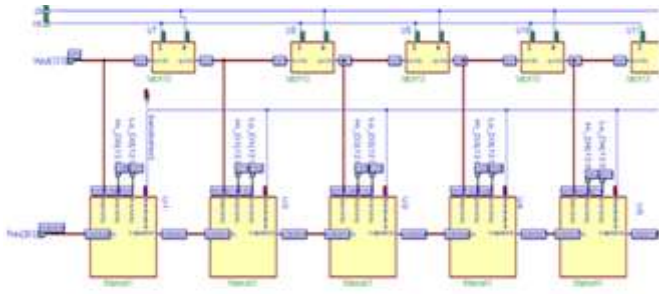


Figure 3: The RTL schematic of filter unit

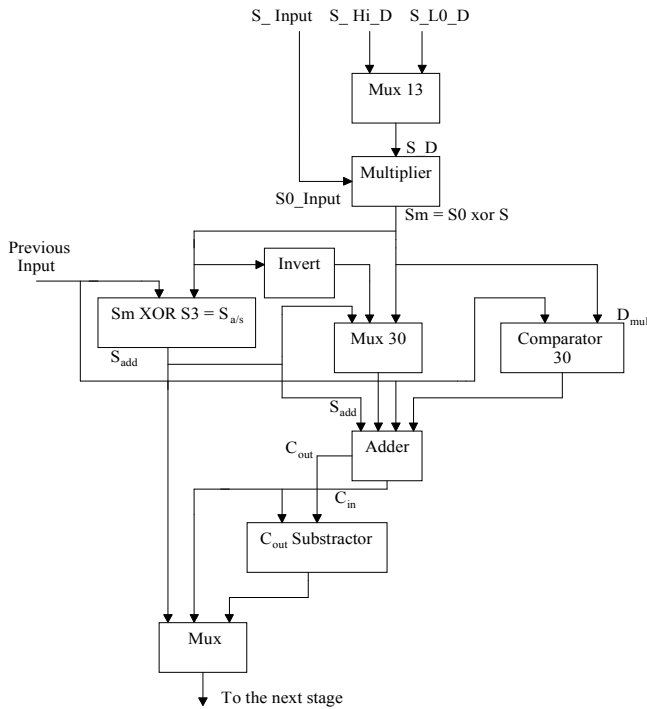


Figure 4: The Proposed Filter Cell

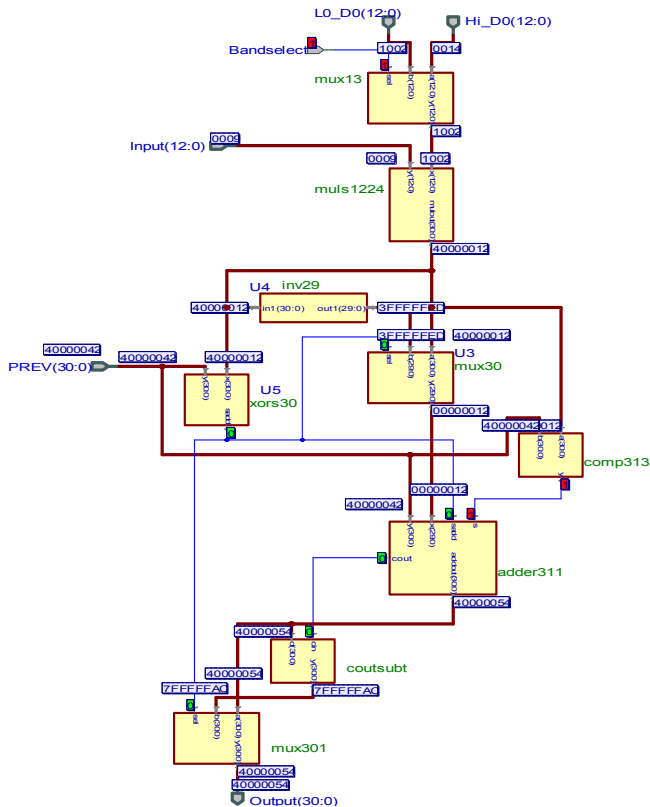


Figure 5: The RTL Schematic of Filter Cell

4.2 The Storage Unit

Two storage units are used in the proposed architecture.

- Input Delay Unit (ID) and
- Register Bank (RB)

Input Delay Unit (ID):

The data registers and input delay used in these storage units have been constructed from standard D-latch. Equations 2a-2n shows that the value of computed filter coefficient depends on the present as well as the five previous data samples. The negative time indexes in Equations 2 correspond to the reference starting time unit 0. Figure 6 shows the block diagram of the input delay unit.

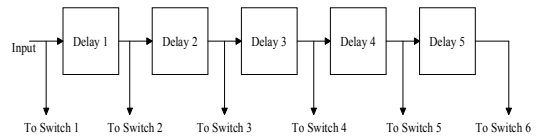


Figure 6: Input Delay Unit (ID)

As shown in figure five delays are connected serially. At any clock cycle each delay passes its contents to its right neighbor which results in only five past values being retained. The input of delays is applied to the switch. The RTL schematic of input delay unit is shown in Figure 7.

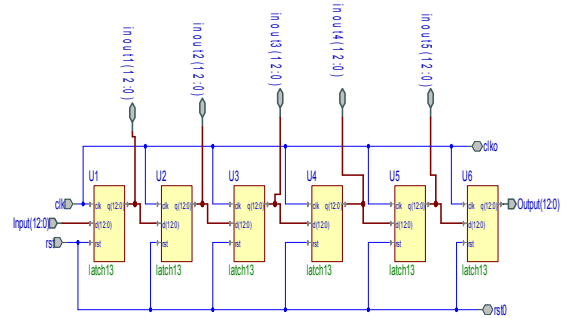


Figure 7: The RTL Schematic of Input Delay Unit

Register Bank (RB):

In proposed architecture number of registers required is 26. Here, two 13 registers architecture are connected serially and constitute one register bank and are controlled by an overall clock. The output of one register is directly connected to the input of the adjacent register, and thus the register bank is implemented as shown in Figure 8 and its RTL schematic is shown in Figure 9.

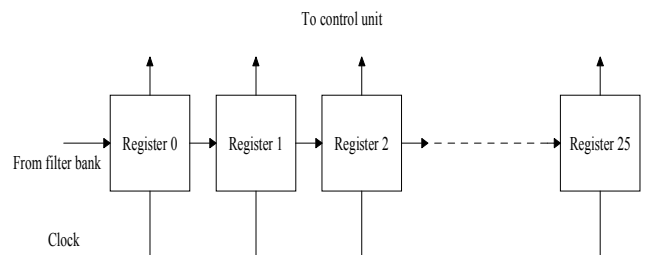


Figure 8: Register Bank (RB)

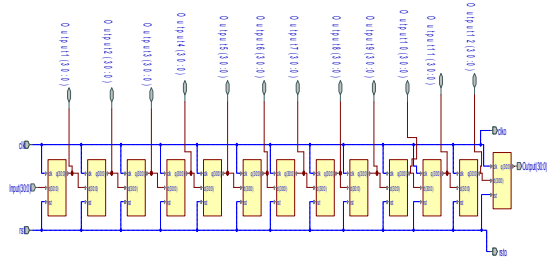


Figure 9:The RTL Schematic of Register Bank (RB)

4.3 Control Unit

In DWT-SA architecture, schedule based on latency of 1 is proposed to meet the real time requirements in some applications. The computations are scheduled at the earliest possible clock cycle, and computed output samples are available one clock cycle after they have been scheduled as shown in Table 1. The delay is minimized through the pipeline facilitating real time operation. The computation schedule in table corresponds to a high hardware utilization of more than 85%. All the intermediate and the associated periods of activity are listed in Table 2.

Table 1: Schedule for one complete set of computations

Cycles	High-pass	Low-pass
1	b(0)	c(0)
2	--	--
3	b(2)	c(2)
4	d(0)	e(0)
5	b(4)	c(4)
6	--	--
7	b(6)	c(6)
8	d(4)	e(4)
9	b(8)	c(8)
10	f(0)	Low-pass

Table 2: Activity periods for intermediate results

Sample	Available Cycles	Life Period
c(0)	1	1 to 12
c(2)	3	3 to 14
c(4)	5	5 to 16
c(6)	7	7 to 18
e(0)	12	12 to 38
e(4)	16	16 to 38

The complete design of the control unit for DWT-SA is shown in Figure 10. The control unit uses switch, decoder, and four FSM. The switching action is done by using FSM. State diagram is used to represent FSM. CU directs data from the Input Delay (ID) or the register bank (RB) to the filter unit (FU). The CU multiplexes data from the ID every second cycle, and from the RB in cycles 4, 6, and 8. In cycle 2, 6, CU remains idle, i.e. it does not allow any passage of data. Proper timing synchronization as well as enabling and disabling of the CU are insured by the CLK signal. The RTL schematic of control unit is shown in Figure 11.

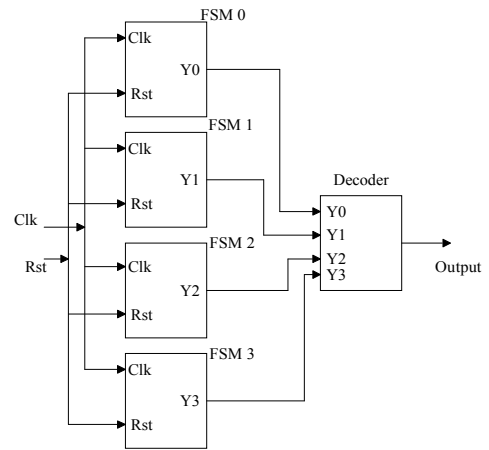


Figure 10: The Control Unit

Control logic consists of four FSM. The switch is operated on this state diagram. According to that it accepts data from input delay and register bank. Figure 12 shows the state diagram for FSM0. Here, there are two states, S1 and S2. When reset is 1, it produces output 1. Otherwise it produces 0.

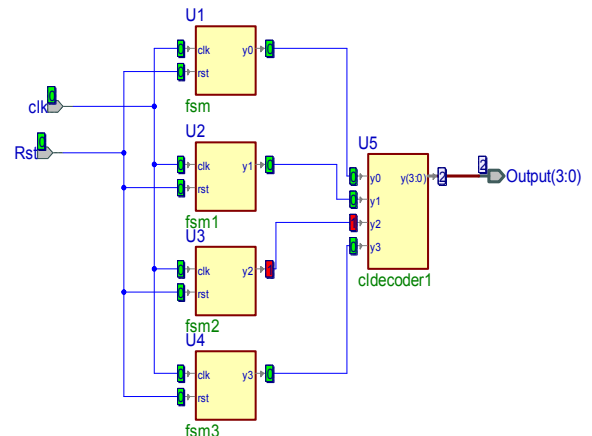


Figure 11: The RTL Schematic of Control Unit

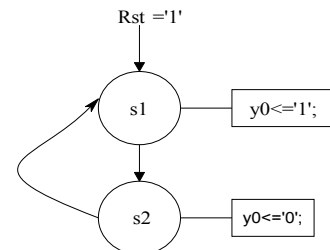


Figure 12: State Diagram for FSM0

Figure 13 shows the state diagram for FSM1. It consists of four states, S1, S2, S3, S4. When reset is 1, and the output is 0 for first clock. After that it goes to the next state, i.e. S2. At that time clock is incremented by 1. When clock cycle is less than 2, it produces output 0. But, when clock is greater than 2 then it goes to the next state. In S3 state, it produces output 1. This process is repeated for clock 3, 4, 5, 6, and 7. If clock is greater than 7 then it again comes to the S3 state and produces the output.

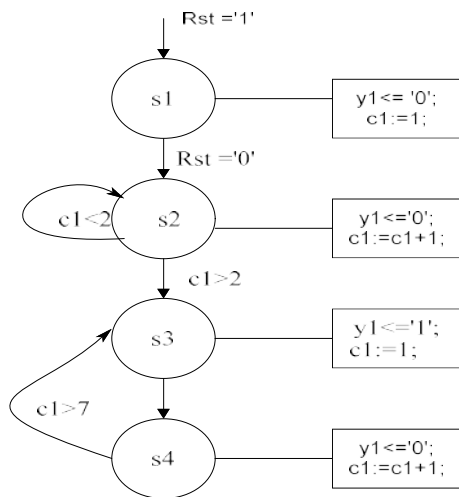


Figure 13: State Diagram for FSM1

Figure 14 shows state diagram for FSM2. When reset is 0, state S2 produces output 0. This occurs when clock is less than 6. For the next clock i.e. Clock is greater than 6, the state S3 produce output 1. But when clock is greater than 7, then state S4 changes its state to the previous state S3.

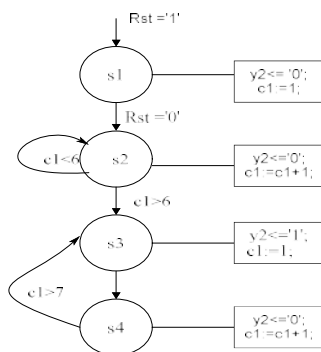


Figure 14: State Diagram for FSM2

The next is FSM3, which consist of S1, S2, S3, and S4. Figure 15 shows the state diagram for FSM3. When reset is 1, output y3 produces 0. In state S2, when clock cycle is less than 8, then output is 0. But in the next clock cycle the output is high. If clock cycle is greater than 7, it changes the state S4 to S3 and produces output high. In all this FSM, outputs are connected to decoder. The output of decoder is connected to the select line of switch, by selecting particular select line; switching action of switch is done. And according to that switch, the data is applied to the filter cell.

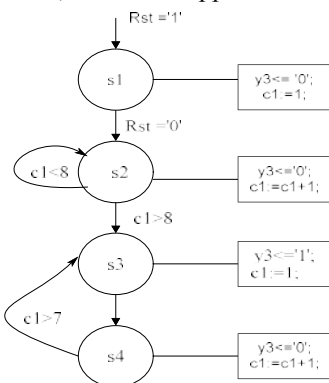


Figure 15: State Diagram for FSM3

5. Register Allocation

In the DWT-SA architecture Control Unit (CU) and the Register Bank (RB) synchronize the availability of operands. There are two schemes which can be employed for this purpose, namely;

- Forward Register Allocation (FRA)
- The Forward-Backward Register Allocation (FBRA)

The FRA method uses a set of registers which are allocated to intermediate data on the first come first serve basis. It does not reassign any registers to other operands once its contents have been accessed. The FBRA scheme is similar, except that once the operand stored has been used; there register is allocated to another operand. The FRA method is simpler, requires less control circuitry and permits easy adaptation of this architecture for coefficient calculation of more than 3 octaves. It results however in less efficient register utilization. In our work we used FRA register allocation.

5.1 FRA Register Allocation

To demonstrate the construction of the register allocation using the FRA approach, we will consider the case of computing the coefficients $c(0)$ and $c(2)$. As shown in Table 3 coefficient $c(0)$ is computed in clock cycle one. Whereas coefficient $c(2)$ is scheduled for computation in cycle 3. These two computed coefficients along with other four; $c(4), c(6), c(8), c(10)$ are needed for the computation of coefficient $e(0)$. According to table $e(0)$ computation is scheduled for cycle 4. However the six coefficients $c(0), c(2), c(4), c(6), c(8), c(10)$ will not be available until cycle 12, and therefore the calculation of $e(0)$ has to be scheduled for cycle $4+N$, or 12. Similarly, coefficient $e(4)$ is computed not in cycle 8, but $8+N$, thus cycle 16. The number of registers needed becomes apparent once one complete frame of computations has been scheduled.

Table 3: FRA Register Allocation

Cycle	Com	R1	R2	R3	R4	R5	R6
1	c(0)						
2		c(0)					
3	c(2)		c(0)				
4	e(0)	c(2)		c(0)			
5	c(4)		c(2)		c(0)		
6	g(0)	c(4)		c(2)		c(0)	
7	c(6)		c(4)		c(2)		c(0)
8	e(4)	c(6)		c(4)		c(2)	
9	c(0)		c(6)		c(4)		c(2)
10		c(0)		c(6)		c(4)	
11	c(2)		c(0)		c(6)		c(4)
12	e(0)	c(2)		c(0)		c(6)	
13	c(4)	e(0)	c(2)		c(0)		c(6)
14	g(0)	c(4)	e(0)	c(2)		c(0)	
15	c(6)		c(4)	e(0)	c(2)		c(0)
16	e(4)	c(6)		c(4)	e(0)	c(2)	
17	c(0)	e(4)	c(6)		c(4)	e(0)	c(2)
18		c(0)	e(4)	c(6)		c(4)	e(0)
19	c(2)		c(0)	e(4)	c(6)		c(4)
20	e(0)	c(2)		c(0)	e(4)	c(6)	
21	c(4)	e(0)	c(2)		c(0)	e(4)	c(6)
22	g(0)	c(4)	e(0)	c(2)		c(0)	e(4)

23	c(6)		c(4)	e(0)	c(2)		c(0)
24	e(4)	c(6)		c(4)	e(0)	c(2)	
25	c(0)	e(4)	c(6)		c(4)	e(0)	c(2)
26		c(0)	e(4)	c(6)		c(4)	e(0)
27	c(2)		c(0)	e(4)	c(6)		c(4)
28	e(0)	c(2)		c(0)	e(4)	c(6)	
29	c(4)	e(0)	c(2)		c(0)	e(4)	c(6)
30	g(0)	c(4)	e(0)	c(2)		c(0)	e(4)
31	c(6)			e(0)	c(2)		c(0)
32	e(4)	c(6)			e(0)	c(2)	
33	c(0)	e(4)	c(6)			e(0)	c(2)
34			e(4)	c(6)			e(0)
35	c(2)			e(4)	c(6)		
36	e(0)	c(2)			e(4)	c(6)	
37	c(4)	e(0)	c(2)			e(4)	c(6)
38	g(0)	c(4)	e(0)	c(2)		e(0)	e(4)

Table 3: FRA Register Allocation (continued)

Cycle	R7	R8	R9	R10	R11	R12	R13
1							
2							
3							
4							
5							
6							
7							
8	c(0)						
9		c(0)					
10	c(2)		c(0)				
11		c(2)		c(0)			
12	c(4)		c(2)		c(0)		
13		c(4)		c(2)		c(0)	
14	c(6)		c(4)		c(2)		
15		c(6)		c(4)		c(2)	
16	c(0)		c(6)		c(4)		
17		c(0)		c(6)		c(4)	
18	c(2)		c(0)		c(6)		
19	e(0)	c(2)		c(0)		c(6)	
20	c(4)	e(0)	c(2)		c(0)		
21		c(4)	e(0)	c(2)		c(0)	
22	c(6)		c(4)	e(0)	c(2)		
23	e(4)	c(6)		c(4)	e(0)	c(2)	
24	c(0)	e(4)	c(6)		c(4)	e(0)	
25		c(0)	e(4)	c(6)		c(4)	e(0)
26	c(2)		c(0)	e(4)	c(6)		
27	e(0)	c(2)		c(0)	e(4)	c(6)	
28	c(4)	e(0)	c(2)		c(0)	e(4)	c(6)
29		c(4)	e(0)	c(2)		c(0)	
30	c(6)		c(4)	e(0)	c(2)		
31	e(4)	c(6)		c(4)	e(0)	c(2)	
32	c(0)	e(4)	c(6)		c(4)	e(0)	
33		c(0)	e(4)	c(6)			e(0)
34	c(2)		c(0)	e(4)	c(6)		
35	e(0)	c(2)		c(0)	e(4)		
36		e(0)	c(2)		c(0)	e(4)	
37			e(0)	c(2)			e(4)
38	c(6)			e(0)	c(2)		

through the registers as described in Table 1. The output coefficients are obtained from the final filter stage. The proposed DWT-SA architecture uses only one filter. The architecture is optimized in hardware by using only a single multiplier and adder set in each filter cell to generate all high pass and low pass coefficients. The coefficients which are present at the output of filter are stored in register. The control logic controls the switching action of switch. The data which are coming from delay input and register bank is controlled by switch. According to the position of switch, one of the data is selected and performs filtering operations. This process is continued up to the 53 clock cycle.

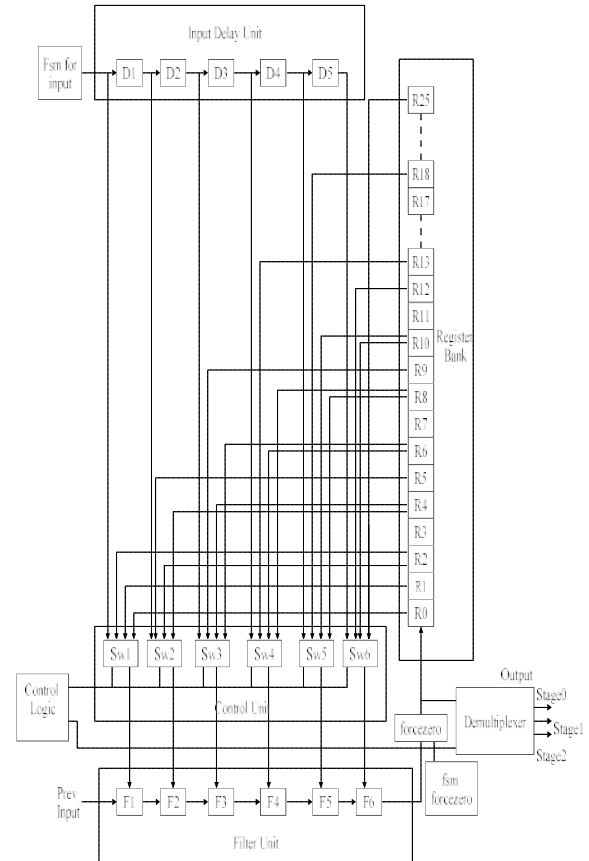


Figure 16: DWT-SA Architecture

To select the particular output coming from filter unit, one of the small unit is used. When select line is zero, it selects one data. Force zero blocks is used to set the values zero. For controlling of this unit FSM is used. The select line is connected to the FSM. When reset is zero, it produces output. Otherwise it produces 0. This results in a simple and efficient systolic implementation for the computation of 1-DWT and hence is suitable for VLSI implementation.

6. DWT-SA Architecture

The proposed architecture is shown in Figure 16 and its RTL schematic is shown in Figure 17. It is obtained by systematic analysis of the FRA register allocation in Table 3 in conjunction with the filter equations 1a and 1a. Delay consist of the DWT-SA architecture consists of the latency period necessary to fill up the filter for the first time, plus the delay

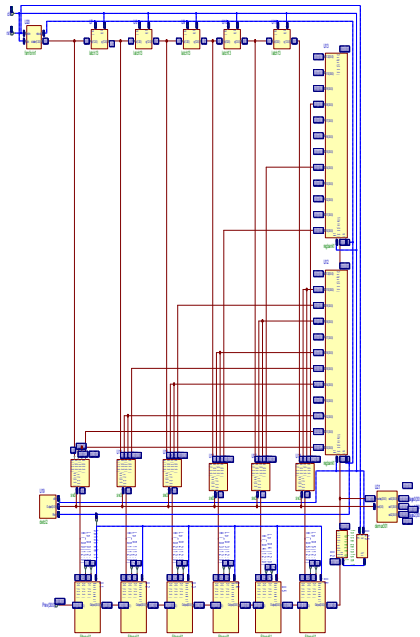


Figure 17: RTL schematic of DWT-SA architecture

The RTL view of DWT-SA for Daubechies3 is shown in Figure 18. This systolic array architecture is designed and implemented using quartus II by device: 'Cyclone;EP2C20F484C7'. Here two elements are used to implement DWT-SA architecture. We get the same RTL view for Haar and Coiflets wavelets

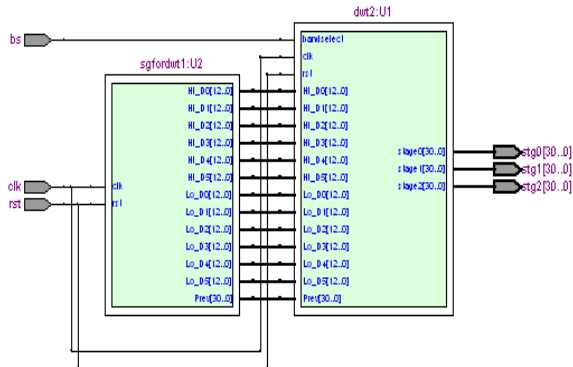


Figure 18: RTL view of DWT-SA for Daubechies3 wavelet

7. Simulation Results of DWT-SA Architecture for Daubechies3, Haar and Coiflets1 Wavelet

MATLAB is the software which is used in our project to verify the result with VHDL simulation. The high pass and low pass coefficients are calculated from MATLAB which are in decimal form. We convert these into binary and padding some zeroes in it. Because the filter cell and multiplexer is designed for 31 bit, 13 bit respectively. Out of this 13 bit, 12 bits are data bits and 1 MSB bit is signed bit. The signed bit represents the positive or negative number. All the implementation and simulation is done in Active HDL 7.1. Simulated waveform gives result for different band select. When band select is '1' the low pass coefficients are selected and gives Approximation coefficients. When band select is '0' the high pass coefficients are selected and gives Details coefficients. The result of DWT-SA is in hexadecimal format.

Table 4 shows low pass coefficients of daubechies3, haar and coiflets1 wavelet in hexadecimal form.

Table 4: Low pass Coefficients of db3, haar and coiflets1 wavelet in Hex form

Low pass coefficients	db3 wavelet	Haar wavelet	coiflets1 wavelet
LO_D0	0001	0012	0000
LO_D1	1002	0012	1002
LO_D2	1003	0	000A
LO_D3	000B	0	0015
LO_D4	0014	0	0008
LO_D5	0008	0	1002

Table 5, Table 6 and Table 7 shows the result in terms of approximation coefficient in hexadecimal form of daubechies3, haar and coiflets1 wavelet.

Table 5: Approximation Coefficients of db3 wavelet

When band select is '1'		
Approximation coefficients of db3		
First stage output	Second stage output	Third stage output
ca1	ca11	ca111
-1	9	-54
7	-42	383
23	161	-6C9
24	51C	7AD8
1C	E0	700
0	0	0

Table 6: Approximation Coefficients of Haar wavelet

When band select is '1'		
Approximation coefficients of Haar		
First stage output	Second stage output	Third stage output
ca1	ca11	ca111
24	510	88B0
24	288	

Table 7: Approximation Coefficients of coiflets1 wavelet

When band select is '1'		
Approximation coefficients of coiflets1		
First stage output	Second stage output	Third stage output
ca1	ca11	ca111
-2	4	-8
1D	B2	-31A
23	531	8065
25	160	-5E
6	-C	18
0	0	0

Table 8 shows high pass coefficients of daubechies3, haar and coiflets1 wavelet in hexadecimal form.

Table 8: High pass coefficients of db3, haar and coiflets1 wavelet in Hex form

High pass coefficients	db3 wavelet	Haar wavelet	coiflets1 wavelet
HO_D0	1008	1012	0002
HO_D1	0014	0012	0008
HO_D2	100B	0	1015
HO_D3	1003	0	000A
HO_D4	0002	0	0002
HO_D5	0001	0	0000

When band select is '0' the high pass coefficients are selected and gives Details coefficients. Table 9, Table 10 and Table 11 shows the result in terms of detail coefficients in

hexadecimal form of daubechies3, haar and coiflets1 wavelet in hexadecimal form.

Table 9: Details coefficients of db3 wavelet

When band select is '0'		
Details coefficients of db3		
First stage output	Second stage output	Third stage output
cd1	cd11	cd111
C	100	1110
-2	05E	086E
1	0BA	114
-B	-1E	75
3	3	3
0	0	0

Table 10: Details coefficients of Haar wavelet

When band select is '0'		
Details coefficients of Haar		
First stage output	Second stage output	Third stage output
cd1	cd11	cd111
0	0	0
0	0	0

Table-11:Details coefficients of coiflets1 wavelet

When band select is '0'		
Details coefficients of coiflets1		
First stage output	Second stage output	Third stage output
cd1	cd11	cd111
-A	4E	34E
-1	6F	9D
1	D5	906
-9	2	4
2	0	0
0	0	0

The Systolic array architecture of DWT is synthesized, placed and routed for cyclone device EP2C20F484C7. The levels of logic cells reported are 8% for Daubechies3, 5% for Haar, 2% for coiflets1. The minimum clock period reported by the synthesis tool after placing and routing is given in Table 12. The Area Analysis reports of each wavelet for Discrete Wavelet Transform Systolic array architecture implementation are given in Table 13.

Table 12: Time Analysis for device EP2C20F484C7

Parameters	Daubechies3	haar	Coiflet1
Clock Period(ns)	53.508 ns	53.743 ns	51.892 ns
Clock Speed(MHz)	18.69 MHz	18.61 MHz	19.27 MHz

Table 13: Area Analysis for device EP2C20F484C7

Parameters	Daubechies3	haar	Coiflet1
Total Logic Elements	1515, 8%	955,5%	1407,2%
Total Combinational Functions	1320, 7%	907,5%	1212,6%
Dedicated Logic Registers	336, 2%	134,1%	336, 2%
LUT-only LCs	1179(1)	821(0)	1071(1)
Register-Only LCs	195(0)	48(0)	195(0)
LUT/Register LCs	141(0)	86(0)	141(0)

For the verification of VLSI results, MATLAB is used. The approximation and detail coefficient are obtained from MATLAB. Figure 19 shows the simulation waveform for approximation coefficients and Figure 20 shows the

simulation waveform for details coefficients for Daubechies3 wavelet.

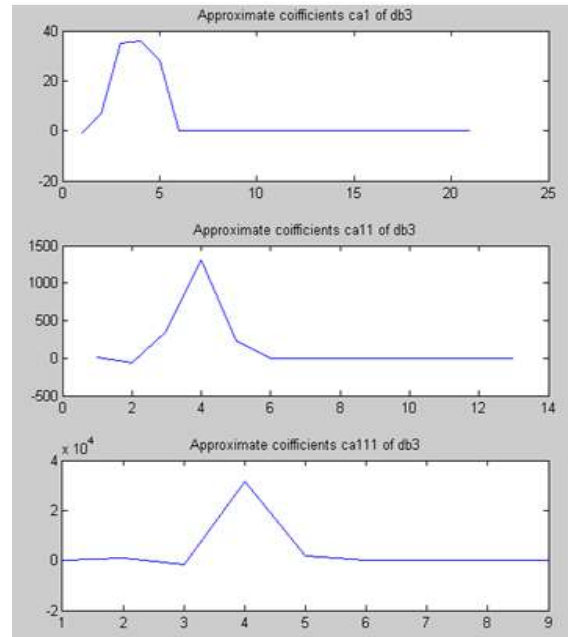


Figure 19: Simulation result of Approximation coefficients for Daubechies3

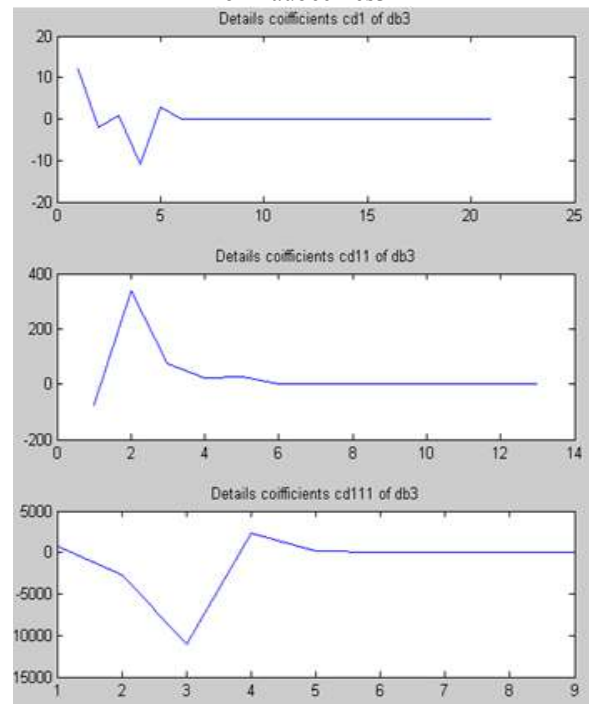


Figure 20: Simulation result of Details coefficients for Daubechies3

Figure 21 and Figure 22 shows the simulation waveform for approximation coefficients and details coefficients of Haar wavelet.

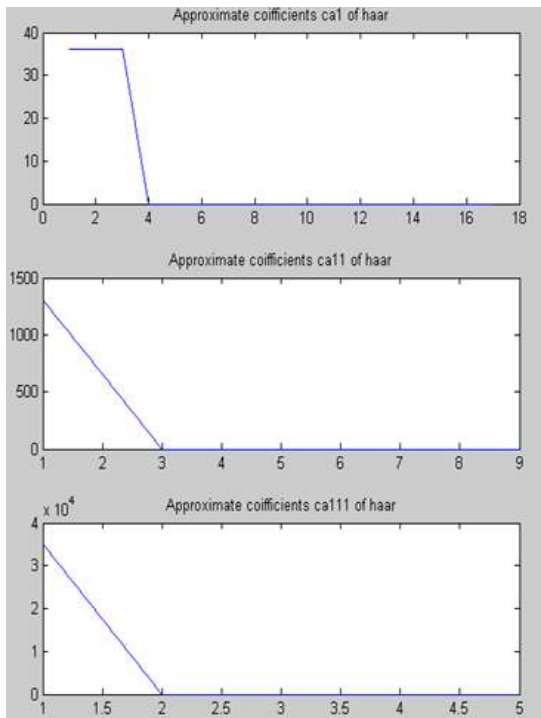


Figure 21: Simulation result of Approximation coefficients for Haar

Also, Figure 23 and Figure 24 shows the simulation waveform for approximation coefficients and details coefficients of Coiflets1 wavelet.

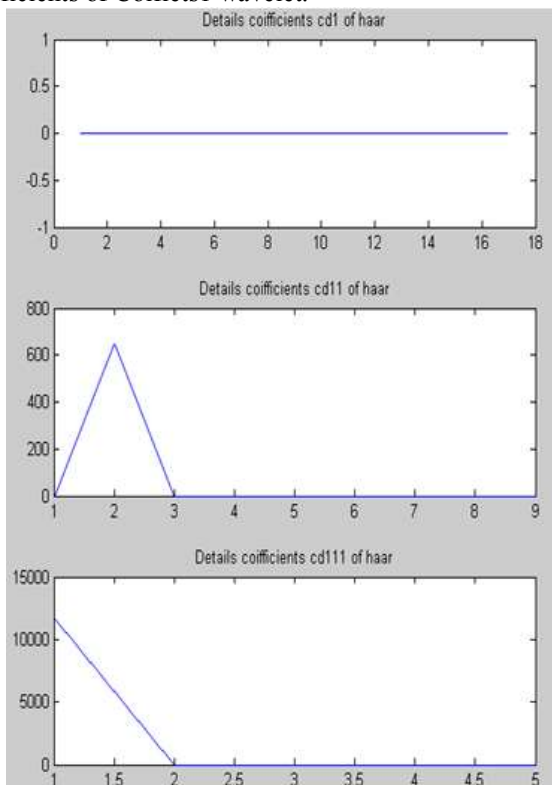


Figure 22: Simulation result of Details coefficients for Haar

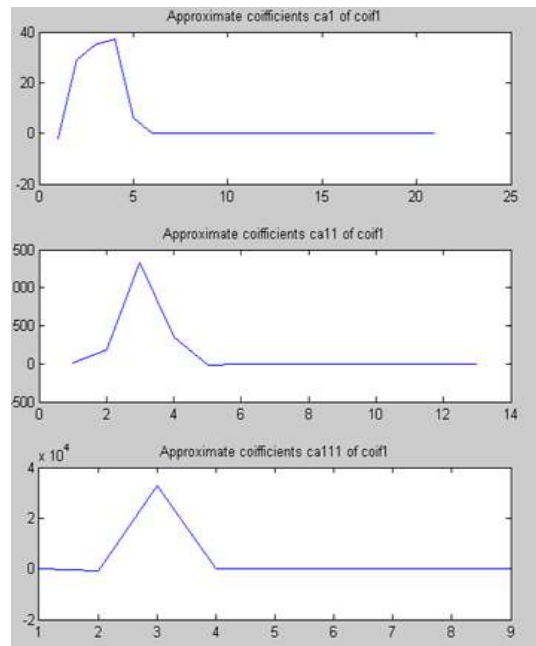


Figure 23: Simulation result of Approximation coefficients for Coiflets1

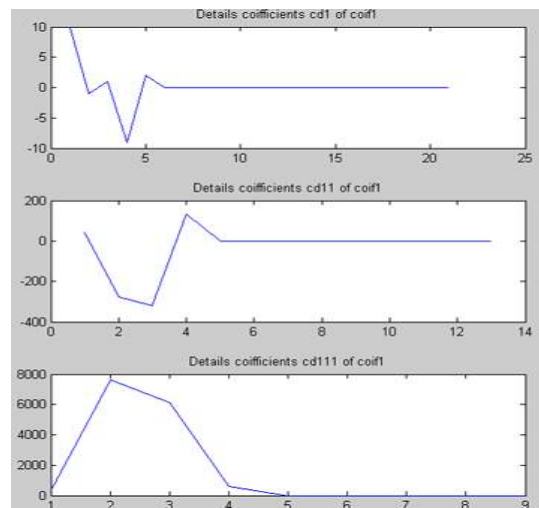


Figure 24: Simulation result of Details coefficients for Coiflets1

8. Conclusion

The proposed DWT-SA architecture computes N coefficients in N clock cycles and achieves real time operation by executing computations of higher octave coefficients in between the first octave coefficient computations. The first octave computations are scheduled for every $N/4$ cycles, while the second and third octaves are scheduled every $N/2$ and N clock cycles respectively.

The main objective of this work is to develop a design resource for designers to implement systolic array architecture of DWT for various wavelets according to the design need such as clock speed, area and time. Systolic array architecture has efficient hardware utilization and it works with data streams of arbitrary size. The design is cascadable, for computation of one, two and three decomposition level. Systolic array Architecture is implemented using Very High Speed Integrated Circuit

(VHSIC) Hardware Description Language (VHDL) and then are simulate using Active HDL.

References

- [1] N. Jayant, "High Quality Networking of Audio-Visual Information", IEEE Communications Magazine, pp. 84-95, September 1993.
- [2] E. A. Fox, "Advances in Interactive Digital Multimedia Systems", IEEE Computer Magazine, pp. 9-21, October 1991.
- [3] P. H. Ang, P. A. Ruetz and D. Auld, "Video Compression Makes Big Gains", IEEE Spectrum Magazine, pp. 16-19, October 1991.
- [4] A. K. Jain, "Image Data Compression: A Review", Proceedings of the IEEE, Vol. 69, No. 3, pp. 349- 389, March 1981.
- [5] K. R. Rao and P. Yip, Discrete Cosine Transform - Algorithms, Advantages, Applications. Academic Press: San Diego, 1990.
- [6] H. G. Musmann, P. Pirsch and H. J. Grailerr, "Advances in Picture Coding", Proceedings of the IEEE, Vol. 73, No. 4, pp. 523-548, April 1985.
- [7] A. bl. Netravali and B. G. Haskell, Digital Pictures, Plenum: New York, 1989.
- [8] FBI Systems Technology Unit: "Gray Scale Fingerprint image Compression Status Report, Nov. 4 1991.
- [9] Chao-Tsung Huang, Po-Chih Tseng, and Liang-Gee Chen," Analysis and VLSI Architecture for 1-D and 2-D Discrete Wavelet Transform", IEEE Transactions on signal processing, vol. 53, No. 4, April 2005
- [10] Chih-Chi Cheng, Chao-Tsung Huang, Ching-Yeh Chen, Chung-JrLian, and Liang-Gee Chen," On-Chip Memory Optimization Scheme for VLSI Implementation of Line-Based Two-Dimensional Discrete Wavelet Transform", IEEE Transactions on circuits and systems for video technology, vol. 17, no. 7, July 2007
- [11] XinTian, Lin Wu, Yi-Hua Tan, and Jin-Wen Tian," Efficient Multi-Input/Multi-Output VLSI Architecture for Two-Dimensional Lifting-Based Discrete Wavelet Transform", IEEE transactions on computers, vol. 60, no. 8, August 2011
- [12] Sze-Wei Lee, Soon-Chieh Lim," VLSI Design of a Wavelet Processing Core", IEEE transactions on circuits and systems for video technology, vol. 16, no. 11, November 2006
- [13] Chao Cheng, Keshab K. Parhi," High-Speed VLSI Implementation of 2-D Discrete Wavelet Transform", IEEE transactions on signal processing, vol. 56, no. 1, January 2008

Author Profile

Ms. RashmiPatil received her B. Eng. Degree in Electronics & Communication from S.S.G.M.C.E. Shegaon, India in 2010 and M.Tech degree in Electronics from R.T.M.N.U. Nagpur, India. Currently she is a research scholar in B.D.C.O.E., Sevagram, India. Her area of interest is applied electronics, VLSI, VHDL, and Low Power optimization.

Dr. M. T. Kolte has completed his B.Tech, M.E., and Ph.D in Electronics and Telecommunication. He is working as Head of Dept.in M.I.T.C.O.E., Pune, India. He has presented and published many papers in National and International Conference.